SORPTION KINETICS AND ISOTHERM STUDIES OF CATIONIC DYES USING GROUNDNUT (*ARACHIS HYPOGAEA*) SHELL DERIVED BIOCHAR A LOW-COST ADSORBENT

JEGAN, J.[1] – PRAVEEN, S.[2*] – BHAGAVATHI PUSHPA, T.[1] – GOKULAN, R.[2]

[1]*Department of Civil Engineering, University College of Engineering Ramanathapuram, Ramanathapuram 623513, Tamil Nadu, India*

[2]*Department of Civil Engineering, G. M. R Institute of Technology, Rajam 532127, Srikakulam District, Andhra Pradesh, India*

**Corresponding author*
e-mail: praveensarvan@gmail.com, praveen.s@gmrit.edu.in; phone: +91-90-4846-3402

(Received 12th Nov 2019; accepted 30th Jan 2020)

Abstract. The removal of a Basic Blue 41 (BB41) and Basic Red 09 (BR09) from an aqueous solution by biochar derived from *Arachis hypogaea* shell (Groundnut shell) was studied. The sorption of cationic dyes (BB41 and BR09) was studied by varying biochar dosage (1–10 g/L), solution pH (3–10), temperature (30 to 50 °C), contact time (0–360 min) and initial dye concentration (25–200 mg/L). At optimum biochar dosages of 2 g/L (BB41) and 1 g/L (BR09), solution pH (8), initial concentration of dye (50 mg/L), and equilibrium time (240 min), groundnut shell derived biochar recorded BB41 and BR09 uptakes of 22.322 and 40.655 mg/g. The kinetic research confirmed that the biosorption rate was quick for groundnut shell-based biochar, and the results were effectively modeled using the Pseudo's first-order and second-order kinetic models. The sorption isotherm studies exhibited that the Sips model provided better results with high correlation coefficients.
Keywords: *biomass, pyrolysis, groundnut, water quality, treatment*

Introduction

Dyes have been used as coloring agents in the textile industries for many years (Wu and Ng, 2008). Different types of dyes are used for diverse applications in the textile manufacturing process; among these, cationic dyes are used the most (Zolliger, 2003).

During the manufacturing of textiles, an enormous quantity of waste sludge and chemically contaminated water are generated. This chemically contaminated wastewater taints the water quality and soil fertility of the affected land cover. Compared to wastewaters released from other industrial applications, those from textile manufacturing are incredibly complex (Gokulan et al., 2019a).

The appearance of colors in the chemically contaminated sewage could be highly visible and harmful even at lower concentrations (Nigam et al., 2000). These polluted wastewaters not only damage the aesthetic nature of the aquatic ecosystem but also affect the photosynthetic activity of aquatic environments by reducing the level of light penetration through it (Kang et al., 2019). These polluted waters contain toxic and carcinogenic substances that must be treated before being discharged into the aquatic systems (Siddique et al., 2017). However, treatment technologies are often not sufficient to remedy these volumes of wastewater (Gokulan et al., 2019b). Since the removal of wastewater is considered as an environmental challenge and mandate of government legislations made in force of these industries to focus on effective treatment of wastewater techniques.

http://www.aloki.hu ● ISSN 1589 1623 (Print) ● ISSN 1785 0037 (Online)
DOI: http://dx.doi.org/10.15666/aeer/1801_19251939

In order to arrest these environmental challenges, various treatment techniques have been used for the removal of dye from wastewater in textile processing units, as insisted by the legislative mandate of government. The most commonly used treatment techniques are Fenton process, photo-Fenton processes (Rosembergue et al., 2019), photoelectro-Fenton (Paz et al., 2020), photo-ferrioxalate (Sankar et al., 2015), reverse osmosis (Sahinkaya et al., 2019), electrochemical oxidation (Nidheesh, 2018), adsorption (Mu et al., 2019), chemical coagulation/flocculation (Beluci et al., 2019).

There are certain disadvantages and limitations of existing dye removal methods in real-time applications. For example, the operating cost of the process is expensive, and they would generate particular wastes that should be treated and disposed of in order to avoid collateral pollution of the environment (Hua et al., 2019). Biological-adsorption can be defined as the uptake of pollutants by inactive biomass through physiochemical treatments (Bhagavathi et al., 2019). Hence adsorption process is viable in dye removal for industrial applications due to its simplicity and sustainability of a broad variety of sorbents that can be used in water treatment (Gupta et al., 2009; Mironyuk et al., 2019).

For this purpose, adsorption by agricultural waste by-products have great potential for removal of different pollutants (Mohebali al., 2019) has proved to be an efficient remediation technique for removing various contaminants such as Dyes (Charola et al., 2018; Wakkel et al., 2019), COD (Mohammad-pajooh et al., 2018) Phenol (da Gama et al., 2018) and heavy metals (Mohammad-pajooh et al., 2018; Liu et al., 2019). In addition to that, agro wastes, by-products are low-cost, available in abundance around the world, renewable resources, eco-friendly, and easy to regenerate (Zhou et al., 2015).

Arachis hypogaea or Groundnut shells are the residual waste produced after the eradication of groundnut seed from its pod. This is a vast agricultural waste with a minor rate of degradation (Zheng et al., 2013). However, groundnut shells have diverse applications such as bioethanol production biodiesel production, carbon nano-sheet formation, and enzyme production. These shells are used as feedstock for biochar preparation, too (Duc et al., 2019). Biochar is a new and popular alternative for the treatment of dye-bearing effluents to selectively isolate dye molecules (Gokulan et al., 2019c). Since the biochar derived from the Groundnut Shell contains various bioactive and different functional compounds, it can be assessed as a feasible bio-sorbent for the adsorptive removal of cationic dyes.

Moreover, the use of groundnut shell derived biochar as a biosorbent in the adsorptive removal of cationic dyes (Basic Blue 41 and Basic red 09) has not been reported, so far. Therefore, in this study, the Groundnut shell derived biochar (GnSB) was examined for the adsorptive removal of Basic Blue 41 (BB41) and Basic Red 09 (BR09) as a model cationic dye and characterized in detail. The influencing parameters of adsorption, including biochar dose, solution pH, initial dye concentration, and temperature, were correlated with the sorption capacity of the biochar. The adsorptive performance of biochar for the removal of BB41 and BR09 was evaluated and modeled.

Materials and methods

Biomass and chemicals

Groundnut shell leftover after the removal of seeds from its pod in the oil mills was used. These shells were obtained from various agro oil processing units in and around Karumathampatti village of Coimbatore city in Tamil Nadu, India. The collected

http://www.aloki.hu ● ISSN 1589 1623 (Print) ● ISSN 1785 0037 (Online)
DOI: http://dx.doi.org/10.15666/aeer/1801_19251939

groundnut shells were used as a feedstock for biochar preparation. These feedstocks were initially washed up with water to remove soil with dust and then exposed to natural sundry for 48 h. Further, the feedstocks were dried up to at 70 °C for 24 h and then pulverized to less than 100 mm for biochar production (Luo et al., 2015). BB41 and BR09 cationic dyes of analytical grade and all other analytical grade chemical agents were obtained from Sigma Aldrich, India. The dye solution was prepared by the dissolution of the required amount of BB41 and BR09 in deionized water. The solution pH of the dye was adjusted to the desired value using 0.1 M HCl or 0.1 M NaOH (Jegan et al., 2016). The chemical structure and characteristics of all the cationic dyes were illustrated in *Figure 1* and *Table 1*.

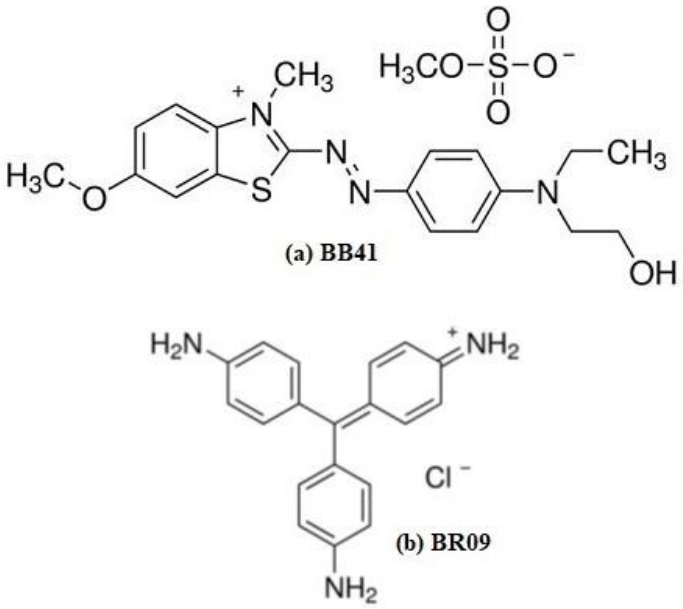

Figure 1. *The structure of cationic dyes Basic Blue 41 (a) and Basic Red 09 (b)*

Table 1. *The characteristics of cationic dyes*

Dyes	Empirical formula	Colour index	Molecular weight (g/mol)	λ max (nm)
Basic Blue 41	$C_{20}H_{26}N_4O_6S_2$	11105	482.57	618
Basic Red 09	$C_{19}H_{17}N_3$ HCl	42500	323.82	546

Pyrolysis of biomass

The biomass of 100 g was kept in a crucible covered with small holes of alumina foil and then flamed at a preferred temperature in a muffle furnace (Mahdi et al., 2017) and maintained it for 120 min in the existing operating conditions under O_2 limited environment (Luo et al., 2015). The heating rate was maintained at 5 °C/min in the pyrolysis, and the resultant biochar was further allowed to cool to room temperature overnight. This experiment was performed at different temperatures (300, 350, 400, 450, and 500 °C) with three trails at each condition to find out the optimum condition. The resultant biochar was moved to a desiccator and further used for various sorption studies.

http://www.aloki.hu ● ISSN 1589 1623 (Print) ● ISSN 1785 0037 (Online)
DOI: http://dx.doi.org/10.15666/aeer/1801_19251939

Characterization of biochar

The Scanning Electron Microscope was used to determine the surface morphological conditions of the biochar using ZEISS- GeminiSEM. Before analysis, all dried biochar samples were coated with a thin layer of gold for electrical conduction. A Fourier Transform Infrared (FTIR) spectrophotometer (Thermo Scientific Ltd., USA & Nicolet 6700) has been used to study the availability of different surface functional groups on the sample. Before these analyses, these dried samples were assorted with KBr to form pellets (Zama et al., 2017).

Adsorption studies

By optimizing the operating parameters with a target to achieve the maximum sorption uptake, batch trial experiments were performed. The biochar dose was added to a 250 mL of Erlenmeyer flask consist of 100 mL of dye concentration, and it was mixed well using an incubated shaker at 200 rpm for 6 h. Then centrifuged for 10 min at 4000 rpm. Finally, the dye concentration was measured from the UV-Spectrophotometer using the supernatant. These adsorption trials were performed for different process conditions.

Isotherm and kinetic studies

In order to determine the maximum dye sorption capacity of the biosorbent, isotherm experiments were carried out by varying the concentrations from 25 to 200 mg/L. The experiment trials were performed at the desired pH, temperature, and adsorbent dosage. The amount of dye sorbed was determined by the differences observed between the amount of dye added to the biomass and the amount present in the supernatant using *Equation 1:*

Biochar uptake: $$Q = \frac{V(C_0 - C_e)}{W} \quad \text{(Eq.1)}$$

The removal efficiency (%) was calculated by using *Equation 2:*

$$\text{Removal efficiency (\%)} = \frac{C_0 - C_e}{C_n} \times 100 \quad \text{(Eq.2)}$$

where Q is the uptake of dye by sorbent mg/g, V is the dye solution volume (L), C_0 is the initial concentration of dye used (mg/L), C_e is the final (equilibrium) concentration of dye remained in the solution (mg/L), and W is the mass of biochar (g).

Four different equilibrium isotherm models were used to fit the experimental data of BB41 and BR09, biosorption onto Groundnut Shell Biochar as given in *Equations 3, 4, 5* and *6* (Ayawei et al., 2017).

Freundlich model:

$$Q = K_F C_e^{\frac{1}{nF}} \quad \text{(Eq.3)}$$

Langmuir model:

$$Q = \frac{Q_{max} b_L C_e}{1 + b_l C_e} \quad \text{(Eq.4)}$$

http://www.aloki.hu ● ISSN 1589 1623 (Print) ● ISSN 1785 0037 (Online)
DOI: http://dx.doi.org/10.15666/aeer/1801_19251939

Sips model:

$$Q = \frac{K_s C_e^{\beta_s}}{1 + a_s C_e^{\beta_s}} \quad \text{(Eq.5)}$$

Toth model:

$$Q = \frac{Q_{max}\, b_T C_e}{[1+(b_T C_e)^{\frac{1}{n_T}}]^{n_T}} \quad \text{(Eq.6)}$$

where Q_{max} is the maximum uptake of dye by the sorbent (mg/g), n_F is the Freundlich exponent, K_F is the coefficient of the Freundlich model (mg/g) (L/mg) $^{1/n_F}$, b_L is the equilibrium coefficient of Langmuir model (L/mg), a_s is the coefficient of Sips model (L/mg), β_s is the exponent of Sips model, K_s is the isotherm coefficient of Sips model (L/g). b_T is the constant of Toth model (L/mg), and n_T is Toth model exponent.

The kinetic models have been utilized to describe the sorption kinetics as provided in the following equations (*Eqs. 7* and *8*):

Pseudo-first-order kinetic model:

$$Q_t = Q_e\,(1 - exp(-k_1 t)) \quad \text{(Eq.7)}$$

Pseudo-second-order kinetic model:

$$Q_t = \frac{Q_e^2 k_2 t}{1 + Q_e k_2 t} \quad \text{(Eq.8)}$$

where Q_t is the dye uptake capacity at any time t (mg/g), Q_e is the equilibrium dye uptake capacity (mg/g), k_1 (1/min) and k_2 (g/mg.min) are the rate constants of the pseudo-first and pseudo-second-order models, respectively.

Results and discussion

Effect of pyrolysis on biomass

The yield of biochar was strongly influenced by the pyrolytic atmosphere. The biochar yield was defined as a weight percentage of the biochar recovered after pyrolysis (Ronsse et al. 2013). *Figure 2* illustrates the pyrolytic temperature influences on biochar yields for the feedstocks. It was evident that the surge in pyrolytic temperature results in decreases the yield of biochar. This was due to more decomposition of residues at higher temperatures. After a cautious assessment of the results presented in *Figure 2*, the maximum biochar yield was obtained at 350 °C was used for further studies.

Characterization of groundnutshell derived biochar

The surface morphological functionalities of the cationic dye bounded biochar derived from the groundnut shell were assessed by the scanning electron microscope, as shown in *Figure 3*. From this figure, it is evident that the groundnut shell surface was

http://www.aloki.hu ● ISSN 1589 1623 (Print) ● ISSN 1785 0037 (Online)
DOI: http://dx.doi.org/10.15666/aeer/1801_19251939

observed to be smooth before pyrolysis, and it is found to be pore and rough after pyrolysis. The surface sites of the biochar after pyrolysis was enlarged and attained more binding action between the cationic dyes onto the biochar. The change in action on the surface of biochar revealed that ion exchange had happened between the adsorbent and adsorbate (Gokulan et al. 2019d) which in turns on adsorption, this adsorption of cationic dyes on the surface of biochar decreases its porosity, as reported (Ahmadi et al., 2012).

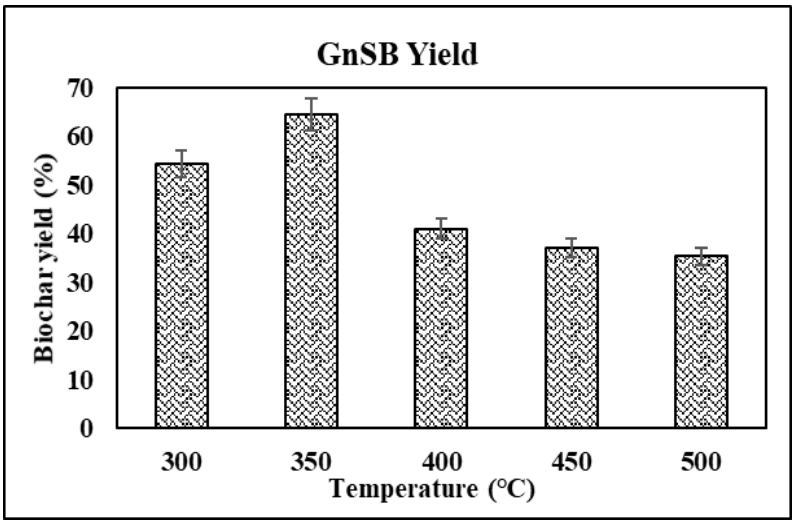

Figure 2. *Effect of pyrolysis temperature on the biochar yield*

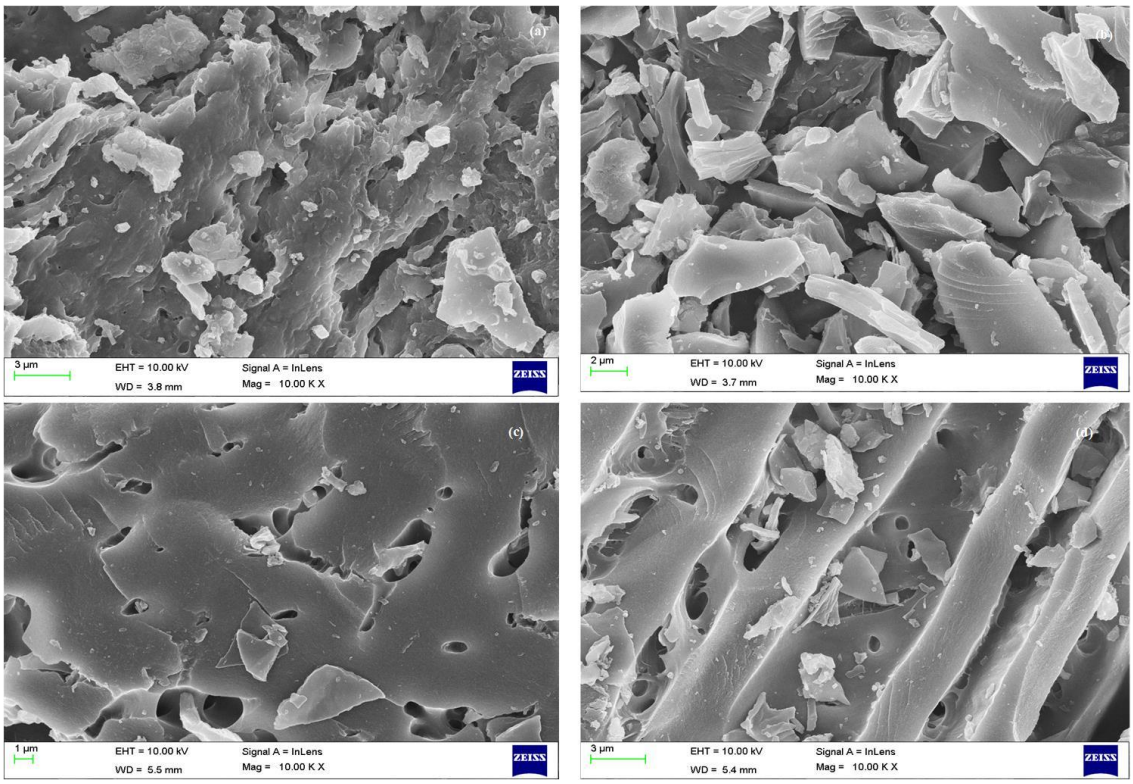

Figure 3. *SEM images of Groundnut Shell (GnS) (a), GnS derived Biochar (GnSB) (b), BB41 bounded GnSB (c) and BR09 bounded GnSB (d)*

http://www.aloki.hu ● ISSN 1589 1623 (Print) ● ISSN 1785 0037 (Online)
DOI: http://dx.doi.org/10.15666/aeer/1801_19251939

In the Energy Dispersive Spectroscopy (EDS) analysis, strong peaks of C, N, O and S are obtained as depicted in *Figure 4.* The results demonstrated that carbon (67.00% to 69.53) and nitrogen (6.13% to 7.31%) content increases and whereas oxygen (26.78% to 23.01%) and sulphur (0.09% to 0.014%) content decreases after pyrolysis. This decrease is due to the decarboxylation and dehydration with subsequent loss of hydroxyl and aliphatic groups.

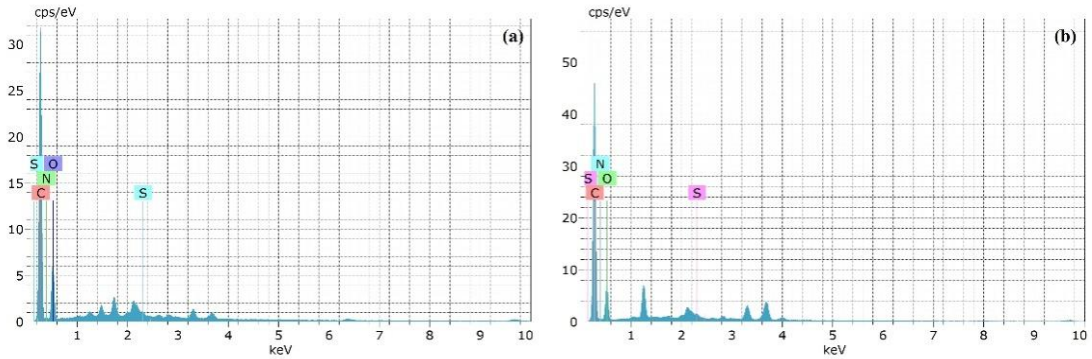

Figure 4. *EDS spectrum of groundnut shell (a) and groundnut shell derived biochar (b)*

The FT-IR spectrum of groundnut shell derived biochar, and cationic dyes bounded biochar are presented in *Figure 5*. The spectrum shows a number of peaks, which indicates the complex nature of the biochars.

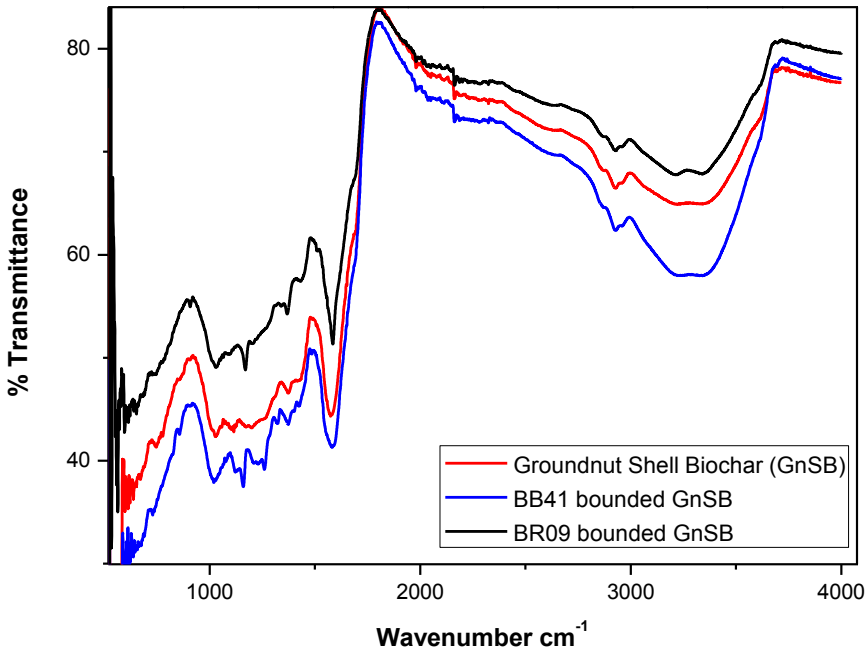

Figure 5. *FT-IR spectra of groundnut shell biochar and basic dyes bounded biochar*

The FT-IR spectrum of biochar barbed out the presence of strong bands at 613 cm^{-1} (C–H (alkynes) band), 744 cm^{-1} (C–H bend), 1114 cm^{-1}(C-O stretch (primary alcohols), 1574 cm^{-1} (C = C stretch, N-H bend) 2928 cm^{-1} (C-H stretch (Alkanes and Alkyls)) and

http://www.aloki.hu ● ISSN 1589 1623 (Print) ● ISSN 1785 0037 (Online)
DOI: http://dx.doi.org/10.15666/aeer/1801_19251939

3339 cm^{-1} (O–H, N-H, stretch). After batch experiments, the biochar spectrum is insignificantly affected by a particular temperature. However, when the BB41 is adsorbed on the biochar surface, several adsorption peak bands are observed at 616, 732, 1160, 1583, 2926, and 3341 $cm^{-1.}$ The peak at 732 cm^{-1} can be indorsed to aromatic compounds (Nasuha et al., 2010). When the BR09 is adsorbed, the peaks are observed at 595, 747, 1170, 1588, 2924, and 3349 cm^{-1}. From the FT-IR spectrum, it is clear that the biochar bounded with cationic dyes revealed the shifts in a functional group, and it is due to the transformation of various ions existent in the active sites of the surface of the adsorbent by dyes sorption. These changes indicate that functional groups on the biochar may be the potential adsorption sites for biosorption of cationic dyes.

Effect of biochar dosage

The influence of biochar dosage is shown in *Figure 6*. Biochar dose was varied from 1 to 10 g/L. From the study, it was evident that the percentage removal increases with an increase in biochar dose and a decrease in dye uptake capacity. For Instance, the removal efficiency of BB41 and BR09 increases from 83.82 to 95.71% and 92.59 to 97.84%, when the dosage increased from 1 to 10 g/L. The experimental rise in efficiency with the surge in biochar dosage could be due to the presence of diversified functional groups and surface sites of the biochar (Slimani et al., 2014). Furthermore, the dye uptake decreases on increasing the biochar dosage. For example, the sorption ability of BB41 and BR09 by groundnut shell derived biochar declined from 41.913 to 4.786 mg/g and 46.299 to 4.892 mg/g, when the biochar dosage increased from 1 to 10 g/L. At low and high sorbent dosages, the dye sorption uptake is greatly affected. Similar results were reported (Vijayaraghavan et al., 2015; Jegan et al., 2016). Comparing the % of removal and dye sorption uptake values, a dose of 2 g/L and 1 g/L, was selected as an optimal dose for BB41 and BR09 for further experiments.

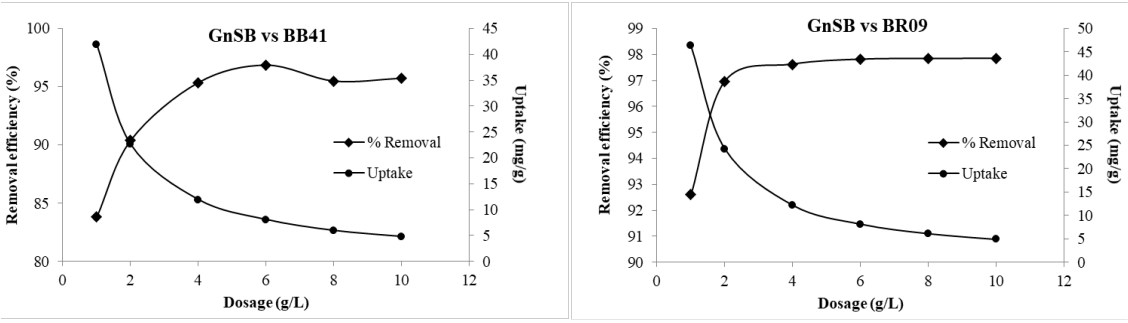

Figure 6. *Effect of biochar dose on the BB41 & BR09 removal efficiency and sorption uptake capacity*

Effect of pH

The pH is the vital parameter which regulates not only the sorption capacity but also the sorption efficiency. With due consideration, the experimental trials were conducted at an optimized biochar dose and desired initial dye concentration of 50 mg/L, the temperature of 35 °C by varying the pH (3-10). *Figure 7* illustrates the influence of pH on dye sorption capacity and the percentage of removal. While varying the pH from 3 to 8, the sorption uptake capacity of groundnut shell derived

http://www.aloki.hu ● ISSN 1589 1623 (Print) ● ISSN 1785 0037 (Online)
DOI: http://dx.doi.org/10.15666/aeer/1801_19251939

biochar onto BB41 and BR09 are increased from 20.01 to 22.60 mg/g and 39.17 to 46.30. Similarly, the percentage of removal also increases from 80.06 to 90.39% and 78.34 to 92.59%, for BB41 and BR09. The initial pH value may influence to increase or decrease the uptake. The increase in the value of pH may decrease the concentration of active H^+ ions, which simultaneously raises the negatively charged sites (Premkumar and Vijayaraghavan, 2015). Due to this negatively charged surface area, the sorption of cationic dye molecules gets increased through electrostatic forces of attraction (Santhi et al., 2016). Comparing the extent of removal and dye sorption capacity values of GnSB favored BR09 followed by BB41. However, the pH value of 8 was taken as optimal for peak performance.

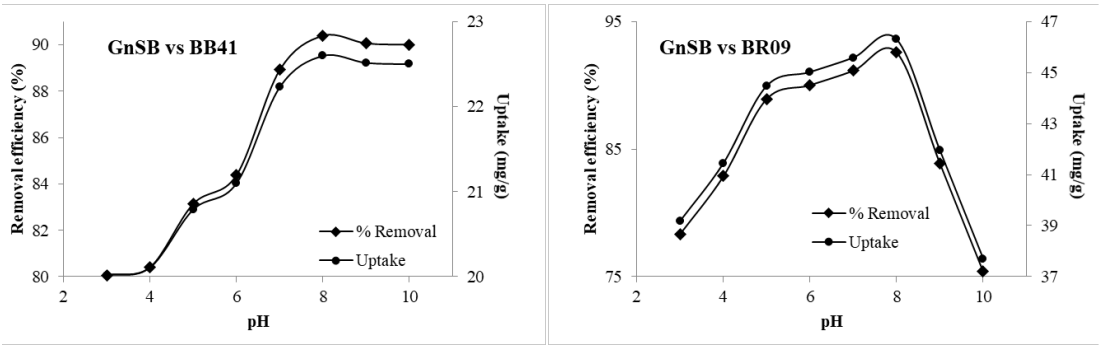

Figure 7. *Effect of solution pH on the BB41 & BR09 removal efficiency and sorption uptake capacity*

Effect of temperature

Figure 8 shows the effect of temperature on the removal efficiency of cationic dyes onto GnSB at different temperatures within the range of 30 to 50 °C at optimized biochar dose and pH with a fixed dye concentration of 50 mg/L were examined. The percentage of BB41 and BR09 removal by GnSB are varying from 90.40 to 80.96% and 92.60 to 77.96%. The surge in temperature accelerates the degree of diffusion of solute and thus strongly influences the uptake capacity of adsorbent towards solutes (Kankilic et al., 2016). While increasing the adsorption temperature of BB41 and BR09 adsorption indicates the fall in uptake capacity. Similar results were reported (Zeng et al., 2006). With this investigation, an ideal temperature of 35 °C has opted for the BB41 and BR09 sorption process.

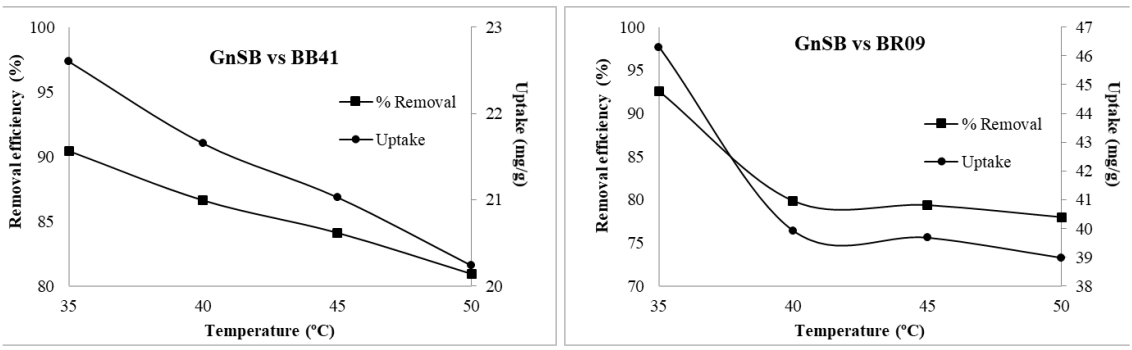

Figure 8. *Effect of adsorption temperature on the BB41 & BR09 removal efficiency and sorption uptake capacity*

http://www.aloki.hu ● ISSN 1589 1623 (Print) ● ISSN 1785 0037 (Online)
DOI: http://dx.doi.org/10.15666/aeer/1801_19251939

Influence of initial dye concentration

The influence of initial dye concentration on the sorption of cationic dyes onto GnSB was experimentally carried out by varying the initial concentration from 25 to 200 mg/L for the optimized biochar dose and pH with ideal temperatures as shown in *Figure 9*. From the experiment data, it was evident that % removal of cationic dyes decreased with a surge in dye concentration. At higher concentrations, the available dye molecules in the solution do not interact with adsorbent binding sites due to the limited number of active sites that become saturated at a certain concentration (Saha et al., 2010). However, the dye sorption capacity at equilibrium condition was increased with a surge in dye concentration. This was due to the initial concentration of the cationic dye, which provides a significant driving force to overcome any mass transfer resistance of the dye between the aqueous and the solid phases (Pirbazari et al., 2014). With due consideration on all these above facts, 50 mg/L was selected as optimal for BB41 and BR09 concentration for GnSB.

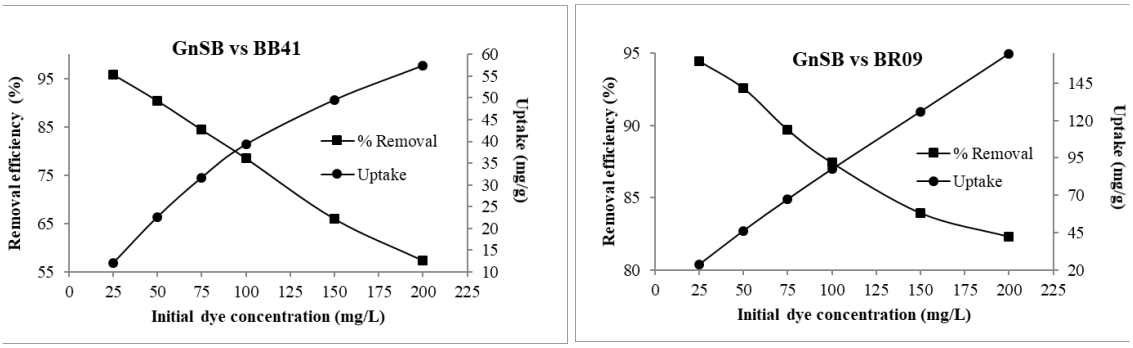

Figure 9. *Effect of initial dye concentration on the BB41 & BR09 removal efficiency and sorption uptake capacity*

Sorption isotherms

The analysis and design of the sorption process require the relevant adsorption equilibrium conditions, which is the most important set of information in understanding an adsorption process. Adsorption equilibrium provides fundamental physiochemical data for evaluating the applicability of the sorption process as a unit operation. By varying the initial concentration of cationic dyes of 25, 50, 75, 100, 150 200 mg/L at optimized pH value and temperature, the adsorption isotherm was determined. From the experiment data, it was seen that sorption potential improved with the increase in initial dye concentration.

To facilitate the adsorption capacities, the equilibrium adsorption models of Freundlich (1906), Langmuir (1916), Sips (1948), and Toth (1971) models were employed. Freundlich and Langmuir are the two-parameter isotherm models, and Sips and Toth are the three-parameter isotherm models used (*Table 2*). In two-parameter isotherms, the Freundlich model was found to be the best-fit isotherm data when compared to other with low correlation coefficient (<0.992) and high % error values, and it can be summarized that K_F and n_F of GnSB were in the following order: BR09 > BB41. The Sips isotherm model has shown a better prophecy of experiments with minimal error and a high correlation coefficient (>0.994) when compared to Toth

http://www.aloki.hu ● ISSN 1589 1623 (Print) ● ISSN 1785 0037 (Online)
DOI: http://dx.doi.org/10.15666/aeer/1801_19251939

isotherm model. BR09 followed by BB41 are provided the maximum constant values for sips model when compared to others.

Sorption kinetics

The sorption kinetics of cationic dyes onto GnSB was carried out by varying the dye concentration from 25 to 200 mg/L at optimized operating parameters until the equilibrium condition attained. The experimental kinetic data indicated that the rate of dye sorption capacity was rapid during the initial hours of the contact, followed by slow attainments in equilibrium. This rapid sorption in the early hours is due to the accessibility of the free functional groups on the biochar surface and, thus, a high concentration gradient that inhibits the system (Zhu et al., 2018). In the same manner on varying initial concentrations of BB41 from 25 to 200 mg/L, equilibrium BB41 uptake capacity of groundnut shell derived biochar increased from 11.40 to 81.27 mg/g. By comparing the different cationic dyes, GnSB exhibited the highest uptake of 164 mg/g for BR09 at 200 mg/L, followed by BB41 (81.27 mg/g).

Table 2. *Isotherm model parameters during adsorption of BB41 and BR09 onto groundnut shell derived biochar*

Models		**BB41**	**BR09**
Langmuir	Q_{Max}	59.888	256.219
	b_L	0.110	0.045
	R^2	0.971	0.984
	% Error	0.380	0.365
Freundlich	K_F	13.838	20.019
	n_F	0.324	0.586
	R^2	0.993	0.998
	% Error	-0.054	0.021
Sips	K_S	13.168	20.251
	β_S	0.494	0.583
	a_S	0.119	0.022
	R^2	0.999	0.998
	% Error	-0.001	0.216
Toth	Q_{Max}	208.881	978.565
	b_T	1.504	0.034
	n_T	4.460	2.747
	R^2	0.996	0.953
	% Error	0.002	0.052

*Q_{max} in mg/g; b_L, b_T in L/mg; K_F in mg/g; $(L/g)^{1/n_F}$;K_S in $(L/g)^{\beta S}$; a_S in $(L/mg)^{\beta S}$

The experimental kinetics are fitted with the Pseudo first order and Pseudo second-order models. The kinetic constants, along with correlation coefficient values, are given in *Table 3.* The first-order model provided the best prediction with an over correlation coefficient of 0.990.

http://www.aloki.hu ● ISSN 1589 1623 (Print) ● ISSN 1785 0037 (Online)
DOI: http://dx.doi.org/10.15666/aeer/1801_19251939

Table 3. *Kinetic parameters of pseudo's model during sorption of cationic dyes onto groundnut shell derived biochar*

Dye	C_o (mg/L)	First-order model				Second-order model			
		q_{eq} (mg/g)	K_1 (1/min)	R^2	% error	q_{eq} (mg/g)	K_2 (1/min)	R^2	% error
BB41	25	11.097	0.364	0.993	0.0031	11.403	0.0861	0.9951	0.001
	50	22.302	0.422	0.995	0.0044	22.873	0.0549	0.9979	0.0048
	75	30.514	0.153	0.996	0.0013	32.399	0.0079	0.9870	-0.070
	100	36.463	0.173	0.996	0.0017	38.474	0.0078	0.9907	-0.044
	150	49.626	0.288	0.996	0.0016	51.839	0.0119	0.9977	-0.066
	200	79.562	0.231	0.996	0.0037	84.368	0.0050	0.9975	-0.001
BR09	25	23.234	0.213	0.993	0.008	24.617	0.0154	0.9931	-0.002
	50	39.626	0.136	0.995	-0.008	42.802	0.0049	0.9873	-0.010
	75	67.388	0.045	0.997	0.014	76.766	0.0007	0.9922	-0.036
	100	82.582	0.104	0.994	0.028	89.996	0.0017	0.9892	-0.013
	150	125.95	0.320	0.994	0.005	129.70	0.0060	0.9958	-0.021
	200	161.11	0.261	0.998	0.005	167.17	0.0033	0.9958	-0.010

Conclusion

The following conclusions are derived from the present study:

a. The biochar derived from groundnut shell biomass at 350 °C through slow pyrolysis was obtained to be the most operative biosorbent.
b. The biosorption capacity of GnSB was sturdily dependent upon the biochar dosage. Experiment trials show that maximum dye sorption capacity was attained at 2 and 1 g/L of biochar dosage for BB41 and BR09 sorption.
c. The solution pH sturdily influences the sorption capacity of GnSB with a pH value of 8 as an optimal condition for the efficient removal of cationic dyes.
d. The SEM and FT-IR analyses exhibited the presence of various functional groups on the surfaces of GnSB.
e. The sorption equilibrium was attained within 240 min, and the biosorption rate was fast. Application of BB41 and BR09 kinetics data disclosed that pseudo's first-order kinetics is better in prediction than the second-order model.
f. According to the Langmuir model, the maximum biosorption capacity of BB41 and BR09 was identified as 59.888 and 256.219 mg/g for GnSB, respectively.
g. From these results, it can be concluded that biochar derived from Ground Shells could be used as a practical bio-based sorbent for the removal of BB41 and BR09 molecules in wastewater.
h. In the future the study may extend in the use of treated or modified biochar for wastewater treatment.

REFERENCES

[1] Ahmadi, S., Chia, C. H., Zakaria, S., Saeedfar, K., Asim, N. (2012): Synthesis of Fe_3O_4 nanocrystals using hydrothermal approach. – Journal of Magnetism and Magnetic Materials 324: 4147-4150.

http://www.aloki.hu ● ISSN 1589 1623 (Print) ● ISSN 1785 0037 (Online)
DOI: http://dx.doi.org/10.15666/aeer/1801_19251939

[2] Ayawei, N., Ebelegi, A. N., Wankasi, D. (2017): Modelling and interpretation of adsorption isotherms. – Journal of Chemistry 2017: 1-11.
[3] Bhagavathi Pushpa, T., Jegan, J., Praveen, S., Gokulan, R. (2019): Biodecolorization of Basic Blue 41 using EM based composts: isotherm and kinetics. – Chemistry Select 4(34): 10006-10012.
[4] Charola, S., Yadav, R., Das, P., Maiti, S. (2018): Fixed-bed adsorption of Reactive Orange 84 dye onto activated carbon prepared from empty cotton flower agro-waste. – Sustainable Environment Research 28(6): 298-308.
[5] De Camargo Lima Beluci, N., Mateus, G. A. P., Miyashiro, C. S., Homem, N. C., Gomes, R. G., Fagundes-Klen, M. R., Vieira, A. M. S. (2019): Hybrid treatment of coagulation/flocculation process followed by ultrafiltration in TiO_2-modified membranes to improve the removal of reactive black 5 dye. – Science of The Total Environment 664: 222-229.
[6] Duc, P. A., Dharanipriya, P., Velmurugan, B. K., Shanmugavadivu, M. (2019): Groundnut shell - a beneficial bio-waste. – Biocatalysis and Agricultural Biotechnology 20: 101206.
[7] Freundlich, H. M. F. (1906): Uber die Adsorption in Lösungen. – Zeitschrift für Physikalische Chemie 57: 385-470.
[8] Gokulan, R., Prabhu, G. G., Jegan, J. (2019a): Remediation of complex remazol effluent using biochar derived from green seaweed biomass. – International Journal of Phytoremediation 21(12):1179-1189.
[9] Gokulan, R., Raja, M. J., Jegan, J., Avinash, A. (2019b): Comparative desorption studies on remediation of remazol dyes using biochar (sorbent) derived from green marine seaweeds. – Chemistry Select 4(25): 7437-7445.
[10] Gokulan, R., Ganesh, P. G., Jegan, J., Avinash, A. (2019c): A critical insight into biomass derived biosorbent for bioremediation of dyes. – Chemistry Select 4(33): 9762-9775.
[11] Gokulan, R., Avinash, A., Ganesh, P. G., Jegan, J. (2019d): Remediation of remazol dyes by biochar derived from Caulerpa scalpelliformis - an eco-friendly approach. – Journal of Environmental Chemical Engineering 7(5): 103297.
[12] Gonçalves, R. G. L., Lopes, P. A., Resende, J. A., Pinto, F. G., Tronto, J., Guerreiro, M. C., Neto, J. L. (2019): Performance of magnetite/layered double hydroxide composite for dye removal via adsorption, Fenton and photo-Fenton processes. – Applied Clay Science 179: 105152.
[13] Gupta, V. K., Carrott, P. J. M., Ribeiro Carrott, Suhas, M. M. L. (2009): Low-cost adsorbents: growing approach to wastewater treatment review. – Critical Reviews in Environmental Science and Technology 39: 783-842.
[14] Hua, P., Sellaoui, L., Franco, D., Netto, M. S., Luiz Dotto, G., Bajahzar, A., Li, Z. (2019): Adsorption of acid green and procion red on a magnetic geopolymer based adsorbent: experiments, characterization and theoretical treatment. – Chemical Engineering Journal 123113.
[15] Jegan, J., Vijayaraghavan, J., Bhagavathi Pushpa, T., Sardhar Basha, S. J. (2016): Application of seaweeds for the removal of cationic dye from aqueous solution. – Desalination and Water Treatment 57(53): 25812-25821.
[16] Kang, D., Kim, K. T., Heo, T. Y., Kwon, G., Lim, C., Park, J (2019): Inhibition of Photosynthetic Activity in Wastewater-Borne Microalgal–Bacterial Consortia under Various Light Conditions. – Sustainability 11: 2951.
[17] Kankiliç, G. B., Metin, A. U., Tuzun, I. (2016): Phragmites australis: an alternative biosorbent for basic dye removal. – Ecological Engineering 86: 85-94.
[18] Langmuir, I. (1916): The constitution and fundamental properties of solids and liquids. Part I. Solids. – Journal of the American Chemical Society 38(11): 2221-2295.
[19] Liu, L., Huang, Y., Zhang, S., Gong, Y., Su, Y., Cao, J., Hu, H. (2019): Adsorption characteristics and mechanism of Pb (II) by agricultural waste-derived biochars produced from a pilot-scale pyrolysis system. – Waste Management 100: 287-295.

http://www.aloki.hu ● ISSN 1589 1623 (Print) ● ISSN 1785 0037 (Online)
DOI: http://dx.doi.org/10.15666/aeer/1801_19251939

[20] Luo, Z., Wang, E., Zheng, H., Baldock, J. A., Sun, O. J., Shao, Q. (2015): Convergent modelling of past soil organic carbon stocks but divergent projections. – Biogeosciences 12: 4373-4383.
[21] Mahdi, Z., Hanandeh, A. E., Yu, Q. (2017): Date seed-derived biochar for Ni (II) removal from aqueous solutions. – MATEC Web of Conferences 120: 05005.
[22] Mironyuk, I. F., Gun'ko, V. M., Vasylyeva, H. V., Goncharuk, O. V., Tatarchuk, T. R., Mandzyuk, V. I., Bezruka, N. A., Dmytrotsa, T. V. (2019): Effects of enhanced clusterization of water at a surface of partially silylated nanosilica on adsorption of cations and anions from aqueous media. – Microporous and Mesoporous Materials 277: 95-104.
[23] Mohammad-pajooh, E., Turcios, A. E., Cuff, G., Weichgrebe, D., Rosenwinkel, K.-H., Vedenyapina, M. D., Sharifullina, L. R. (2018): Removal of inert COD and trace metals from stabilized landfill leachate by granular activated carbon (GAC) adsorption. – Journal of Environmental Management 228: 189-196.
[24] Mohebali, S., Bastani, D., Shayesteh, H. (2019): Equilibrium, kinetic and thermodynamic studies of a low-cost biosorbent for the removal of Congo red dye: acid and CTAB acid modified celery (Apium graveolens). – Journal of Molecular Structure 1176: 181-193.
[25] Mu, N., Alqadami, A. A., AlOthman, Z. A., Alsohaimi, I. H., Algamdi, M. S., Aldawsari, A. M. (2019): Adsorption kinetics, isotherm and reusability studies for the removal of cationic dye from aqueous medium using arginine modified activated carbon. – Journal of Molecular Liquids 293: 111442.
[26] Nasuha, N., Hameed, B. H., Din, A. T. M. (2010): Rejected tea as a potential low-cost adsorbent for the removal of methylene blue. – Journal of Hazardous Materials 175: 126-132.
[27] Nidheesh, P. V., Zhou, M., Oturan, M. A. (2018): An overview on the removal of synthetic dyes from water by electrochemical advanced oxidation processes. – Chemosphere 197: 210-227.
[28] Nigam, P., Armour, G., Banat, I. M., Singh, D., Marchant, R. (2000): Physical removal of textile dyes and solid-state fermentation of dye adsorbed agricultural residues. – Bioresource Technology 72(3): 219-226.
[29] Paz, E. C., Pinheiro, V. S., Sousa Joca, J. F., Sotana de Souza, R. A., Gentil, T. C., Lanza, M. R. V., de Oliveira, H. P. M., Pereira Neto, A. M., Gaubeur, I., Santos, M. C. (2020): Removal of Orange II (OII) dye by simulated solar photoelectro-Fenton and stability of WO2.72/Vulcan XC72 gas diffusion electrode. – Chemosphere 239: 124670.
[30] Pirbazari, A. E., Saberikhah, E., Badrouh, M., Emami, M. S. (2014): Alkali treated Foumanat tea waste as an efficient adsorbent for methylene blue adsorption from aqueous solution. – Water Resources and Industry 6: 64-80.
[31] Premkumar, Y., Vijayaraghavan, K. (2015): Biosorption potential of coco-peat in the removal of methylene blue from aqueous solutions. – Separation Science and Technology 50: 1439-1446.
[32] Ronsse, F., van Hecke, S., Dickinson, D., Prins, W. (2013): Production and characterization of slow pyrolysis biochar: influence of feedstock type and pyrolysis conditions. – GCB Bioenergy 5(2): 104-115.
[33] Saha, P., Chowdhury, S., Gupta, S., Kumar, I. (2010): Insight into adsorption equilibrium, kinetics and thermodynamics of malachite green onto clayey soil of Indian origin. – Chemical Engineering Journal 165: 874-882.
[34] Sahinkaya, E., Tuncman, S., Koc, I., Guner, A. R., Ciftci, S., Aygun, A., Sengul, S. (2019): Performance of a pilot-scale reverse osmosis process for water recovery from biologically-treated textile wastewater. – Journal of Environmental Management 249: 109382.
[35] Sankar, C., Lokesh, D., Moholkar, V. S. (2015): Dye decolorization with hybrid advanced oxidation processes comprising sonolysis/Fenton-like/photo-ferrioxalate

http://www.aloki.hu ● ISSN 1589 1623 (Print) ● ISSN 1785 0037 (Online)
DOI: http://dx.doi.org/10.15666/aeer/1801_19251939

systems: a mechanistic investigation. – Separation and Purification Technology 156 (2): 596-607.
[36] Santhi, T., Manonmani, S., Vasantha, V. S., Chang, Y. T. (2016): A new alternative adsorbent for the removal of cationic dyes from aqueous solution. – Arabian Journal of Chemistry 9(1): S466-S474.
[37] Siddique, K., Rizwan, M., Shahid, M. J., Ali, S., Ahmad, R., Rizvi, H. (2017): Textile Wastewater Treatment Options: A Critical Review. – In: Anjum, N., Gill, S., Tuteja, N. (eds.) Enhancing Cleanup of Environmental Pollutants 2: 183-207.
[38] Sips, R. (1948): On the structure of a catalyst surface. – The Journal of Chemical Physics 16: 490-495.
[39] Slimani, R., Ouahabi, I., E., Abidi, F., Haddad, M. E., Regti, A., Laamari, M. R., Antri, S. E., Lazar, S. (2014): Calcined eggshells as a new biosorbent to remove basic dye from aqueous solutions: Thermodynamics, kinetics, isotherms and error analysis. – Journal of Taiwan Institute of Chemical Engineers 45:578-1587.
[40] Toth, J. (1971): State equation of the solid gas interface layer. – Acta Chimica (Academiae Scientiarum) Hungaricae 6: 311-317.
[41] Vijayaraghavan, J., Bhagavathi Pushpa, T., Sardhar Basha, S. J., Vijayaraghavan, K., Jegan, J. (2015): Evaluation of red marine alga Kappaphycus alvarezii as biosorbent for methylene blue: Isotherm, kinetic and mechanism studies. – Separation Science and Technology 50: 1-7.
[42] Villar da Gama, B. M., do Nascimento, G. E., Silva Sales, D. C., Rodríguez-Díaz, M. M., de Menezes Barbosa, C. M. B., Bezerra Duarte, M. M. M. (2018): Mono and binary component adsorption of phenol and cadmium using adsorbent derived from peanut shells. – Journal of Cleaner Production 201: 219-228.
[43] Wakkel, M., Khiari, B., Zagrouba, F. (2019): Textile wastewater treatment by agro-industrial waste: equilibrium modeling, thermodynamics and mass transfer mechanisms of cationic dyes adsorption onto low-cost lignocellulosic adsorbent. – Journal of the Taiwan Institute of Chemical Engineers 96: 439-452.
[44] Wu, C. H., Ng, H. Y. (2008): Degradation of C. I. Reactive Red 2 (RR2) using ozone-based systems: comparisons of decolorization efficiency and power consumption. – Journal of Hazardous Materials 152: 120-127.
[45] Zama, E. F., Zhu, Y. G., Reid, B. J., Sun, G. X. (2017): The role of biochar properties in influencing the sorption and desorption of Pb (II), Cd (II) and as (III) in aqueous solution. – Journal of Cleaner Production 148: 127-136.
[46] Zeng, G., Zhang, C., Huang, G., Yu, J., Wang, Q., Li, J., Xi, B., Liu, H. (2006): Adsorption behavior of bisphenol A on sediments in Xiangjiang River, Central-south China. – Chemosphere 65: 1440-1499.
[47] Zheng, W., Phoungthong, K., Lü, F., Shao, L. M., He, P. J. (2013): Evaluation of a classification method for biodegradable solid wastes using anaerobic degradation parameters. – Waste Management 33(12): 2632-2640.
[48] Zhou, Y., Zhang, L., Cheng, Z. (2015): Removal of organic pollutants from aqueous solution using agricultural wastes: a review. – Journal of Molecular Liquids 212:739-762.
[49] Zhu, Y., Yi, B., Yuan, Q., Wu, Y., Wang, M., Yan, S. (2018): Removal of methylene blue from aqueous solution by cattle manure-derived low-temperature biochar. – RSC Advances 8(36): 19917-19929.
[50] Zolliger, H. (2003): Color chemistry-syntheses, properties, and applications of organic dyes and pigments. – Verlag Helvetica Chimica Acta, Wiley-VCH, Germany.

http://www.aloki.hu ● ISSN 1589 1623 (Print) ● ISSN 1785 0037 (Online)
DOI: http://dx.doi.org/10.15666/aeer/1801_19251939